Development of Mass Spectrometric Glycan Characterization Tags using Acid-Base Chemistry and/or Free Radical Chemistry

Rayan Murtada, Shane Finn, Jinshan Gao*

Department of Chemistry and Biochemistry, Montclair State University, 1 Normal Avenue, Montclair, NJ 07043, USA

ABSTRACT: Despite recent advances in glycomics, glycan characterization still remains an analytical challenge. Accordingly, numerous glycan-tagging reagents with different chemistries were developed, including those involving acid-base chemistry and/or free radical chemistry. Acid-base chemistry excels at dissociating glycans into their constituent components in a systematic and predictable manner to generate cleavages at glycosidic bonds. Glycans are also highly susceptible to depolymerization by free radical processes, which is supported by results observed from electron-activated dissociation (ExD) techniques. Therefore, the free radical activated glycan sequencing (FRAGS) reagent was developed so as to possess the characteristics of both acid-base and free radical chemistry, thus generating information-rich glycosidic bond and cross-ring cleavages. Alternatively, the free radical processes can be induced via photodissociation of the specific carbon-iodine bond which gives birth to similar fragmentation patterns as the FRAGS reagent. Furthermore, the methylated-FRAGS (Me-FRAGS) reagent was developed to eliminate glycan rearrangements by way of a fixed charged as opposed to a labile proton, which would otherwise yield additional, yet unpredictable, fragmentations including internal residue losses (IRL) or multiple external residue losses (M-ERL). Lastly, to further enhance glycan enrichment and characterization, solid-support FRAGS was developed.

INTRODUCTION

Glycosylation is one of the most common and important post-translational modifications on proteins that play a vital role in biochemical systems.[1] Glycan significantly influence protein folding, activity, stability, solubility, trafficking, localization, oligomerization, and often have intimate involvement in intercellular and intracellular interactions.[2] Alterations of glycan structures have been found in various diseases, such as cancer metastasis, Alzheimer's disease, inherited diseases, pathogen-host interactions, and immune recognition.[3-7] Therefore, profiling disease-associated glycans is essential for the understanding of their functions and mechanisms at the biomolecular level, while also facilitating the identification of diagnostic glycan biomarkers and better design of therapeutic drugs. However, unlike DNA, RNA, and proteins, which possess a predominantly linear structure comprised of a limited number of subunits with a defined stereochemistry, glycans may exhibit incredibly complicated branched structures with a large number of subunits having both structural and stereochemical diversity (**Figure 1**). Moreover, glycosylation is difficult to control as slight condition differences can lead to major glycan structural changes. Furthermore, complete structural characterization requires information regarding linkage, sequence, branching, and anomeric configuration. As a result, glycomics is far less developed than its siblings, genomics, and proteomics.

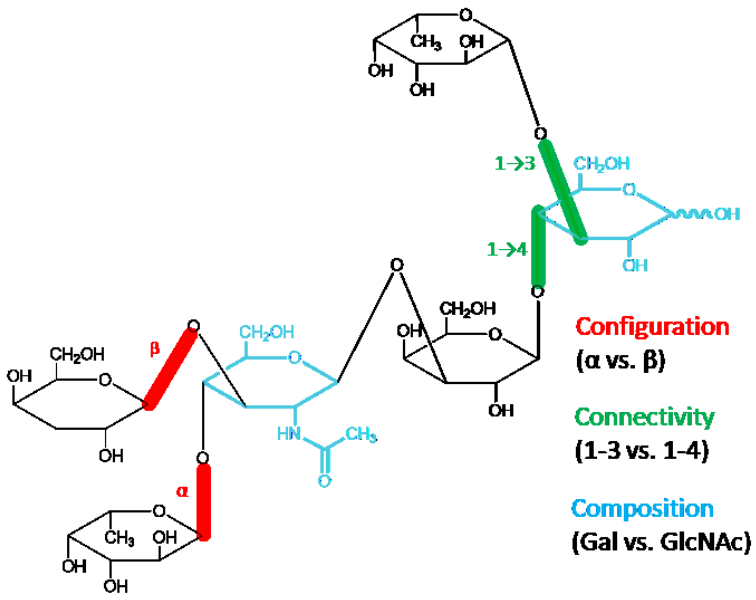

Figure 1. An example of the isomeric heterogeneity of glycans can be represented by the subtle differences in configuration, connectivity, and composition.

Many techniques including high-performance liquid chromatography (HPLC),[8-10] electrophoresis,[11,12] ion mobility,[13-17] and nuclear magnetic resonance (NMR),[18,19] have been employed for glycan structural analysis. However, each of these methods has its limitations. HPLC, electrophoresis, and ion mobility require well-characterized glycan standards. Currently, glycan structure elucidation by these techniques is impeded by the lack of well-characterized glycan standards with structural and stereochemical diversity. NMR requires relatively large quantities of a highly pure sample, and interpretation of NMR spectra is difficult due to the similar chemical environments of many protons and carbons. Mass spectrometry, noted for its minimal sample consumption, high sensitivity, and short acquisition time, has been widely employed for the structural characterization of glycans. Moreover, because mass spectrometers can perform tandem mass spectrometry (MS^n) analysis, they have been used extensively as indispensable tools for glycan structural analysis. Low-energy collision-induced dissociation (CID) typically generates glycosidic bond cleavage when applied to glycans.[20-24] Infrared multiphoton dissociation (IRMPD), another slow-heating fragmentation method, gives results similar to low-energy CID.[25,26] High-energy CID[27], stepped collision energy/higher-energy collisional dissociation (sceHCD)[28,29], and vaccum ultraviolet multiphoton dissociation[30-33] are unavailable on many modern instruments, even though they can generate more cross-ring cleavages than low-energy CID and IRMPD. More recently, electron-activated dissociation (ExD) techniques such as electron capture dissociation (ECD),[21,34-37] electron detachment dissociation (EDD),[38,39] and electron transfer dissociation (ETD)[24,40-43], and electronic excitation dissociation[10,44-46] (EED) have demonstrated the capability of providing extensive and complementary information about glycan structures. Another development in glycopeptidomics in recent years is the use of electron transfer/higher-energy collisional dissociation (EThcD) [47-49] techniques together to provide considerable information about intact structures and locations of glycosylation sites. Mechanisms for ExD methods have been proposed, all of which involve radical-driven fragmentation processes accompanied by complex hydrogen migration and rearrangement. With most ExD methods, the fragmentation efficiency is often relatively low, and cross-ring cleavages are unsystematic and unpredictable due to the absence of well-defined sites for radical generation. Nonetheless, such approaches require special instrumentation to allow interactions between electrons and the targeted ions.

ACID-BASE CHEMISTRY

In contrast to the often unpredictable and unsystematic dissociation pathways associated with the above techniques, natural enzymes excel at depolymerizing glycans into their constituent components in a systematic and predictable manner. This is accomplished by taking advantage of acid-base catalysis to achieve the selective cleavage of the glycosidic bond. In fact, the enzymatic structural analysis of glycans employing a set of highly specific exoglycosidases, sequentially or in a matrix array, has proven to be a powerful analytical tool for the determination of the sequence, the linkage type, and the anomeric configuration.[50] However, this method requires highly pure samples, fully completed hydrolysis, maintenance of optimal enzymatic conditions, and lengthy enzymatic incubation periods. The impact of these natural enzymes throughout glycan analysis provides an impetus to develop biomimetic reagents that, when combined with MS, attempt in part to replicate their chemistry while eliminating the shortcomings of a purely enzymatic approach to glycan sequencing. To mimic the highly selective cleavage and the importance of acid-base chemistry at the active site of natural enzymes during the process of enzymatic glycan depolymerization, reagents such as 2-aminobenzoic acid (2-AA) and 2-aminobenzamide (2-AB) (Figure 2) have been developed and commercialized for glycan quantitation and characterization.[51-53] Collisional activation of the protonated glycans labeled with 2-AA and 2-AB generates cleavages at glycosidic bonds, resulting in B-type and Y-type ions. However, hexose rearrangements were observed upon collisional activation. Meanwhile, Beauchamp and Gao et al. have developed a sequestered proton reagent for acid-catalyzed glycan sequencing (PRAGS; Figure 2) that derivatizes the reducing terminus of glycans with a pyridine moiety possessing moderate proton affinity.[54] Similarly, the gas-phase collisional activation of singly-protonated PRAGS-derivatized maltoheptaose generates extensive Y ions, (Figure 3) which is quite different from the CID of $[M+Metal]^+$,[47] $[M_{permethylated} + Na]^+$,[17] $[M - H + Cl]^{2-}$,[19] and $[M - 2H]^{2-}$ glycans,[12] wherein not only the Y ions but also the A, B, C, X, and Z ions are observed. In particular, the Y ions provide composition and sequence information for the structural analysis of maltoheptaose. Collisional activation on the singly-protonated PRAGS-derivatized highly branched model glycan (Figure 4) mainly generates not only the systematic Y ions but also the Y+Y ions which are generated via a pair of C1–O glycosidic bond cleavages. Moreover, glycan rearrangement ions resulting from the internal residue loss (IRL), and multiple external residue losses (M-ERL) are formed. As shown in Figure 4, $Y_{3HL}+Y_{2H}$ and $Y_{3HH}+Y_{2H}$ are IRL ion resulting from the internal loss of N-acetylglucosamine, and $Y_{1L}+Y_{1H}$, $Y_{1L}+Y_{3HH}$, $Y_{1L}+Y_{3HL}$, $Y_{3HL}+Y_{3HH}$, and $Y_{1L}+B_{2H}$ are M-ERL ions due to simultaneous cleavages of two glycosidic bonds.[48,49] These rearrangement ions are proposed to be initiated by the labile proton and pose a potential problem for the structure determination of the unknown glycans.

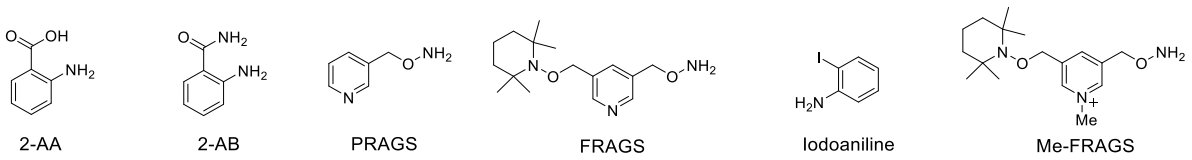

Figure 2. Reagents previously and currently used for glycan analysis: 2-aminobenzoic acid (2-AA), 2-aminobenzamide (2-AB), proton reagent for acid-catalyzed glycan sequencing (PRAGS), free radical-activated glycan sequencing (FRAGS), iodoaniline, and methylated free radical activated glycan sequencing reagent (Me-FRAGS).

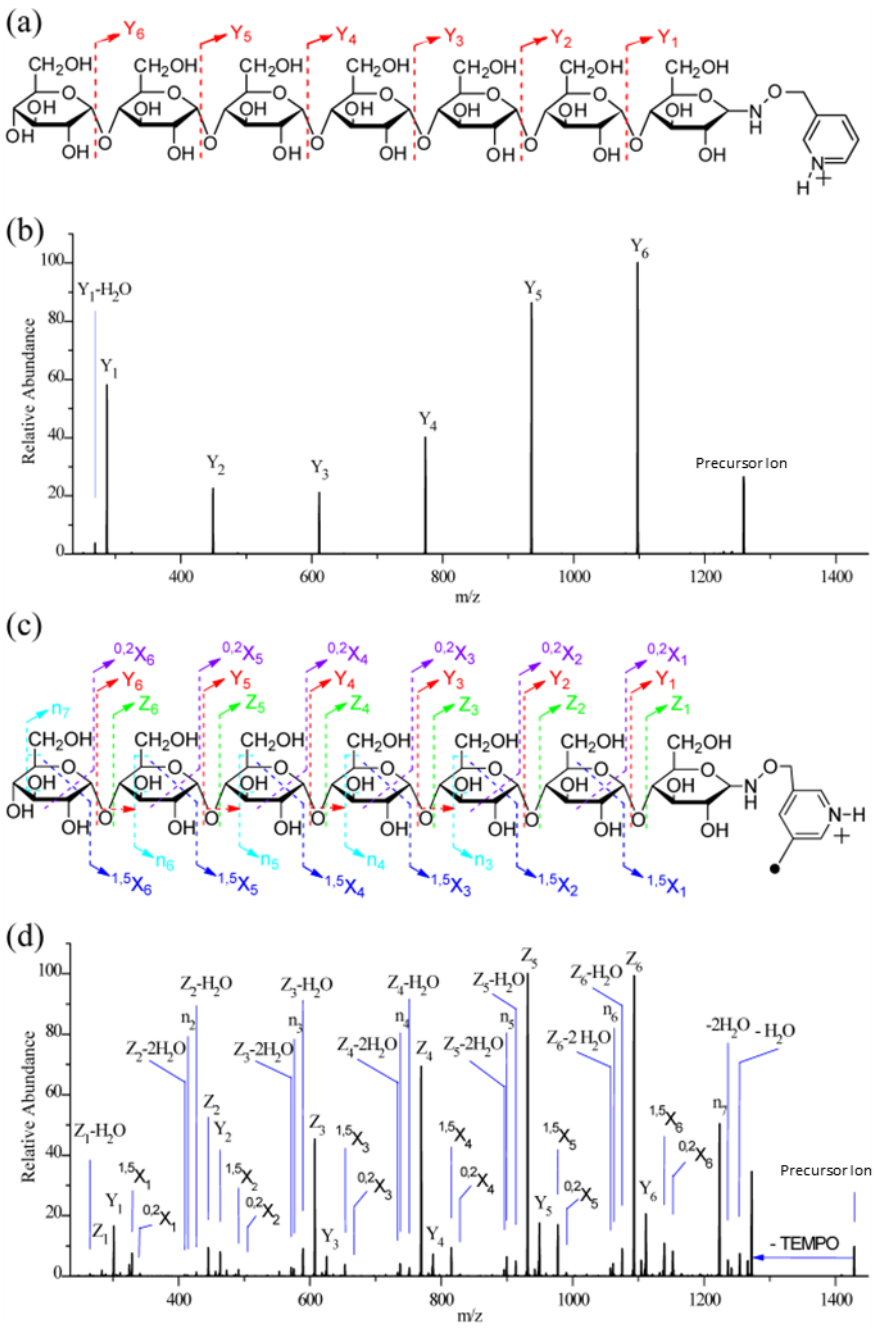

Figure 3. The fragmentation patterns observed following the CID of the singly-protonated PRAGS-derivatized maltoheptaose (a), the CID spectra of singly-protonated PRAGS-derivatized maltoheptaose (b), the fragmentation patterns observed following the CID of the singly-protonated FRAGS-derivatized maltoheptaose (c), and the CID spectra of singly-protonated FRAGS-derivatized maltoheptaose (d),. Precursor ion refers to the protonated molecular ion. The possible fragmentation of the reducing terminus glycan subunit is not observed due to the low mass cut-off (Gao *et al.*, 2013).

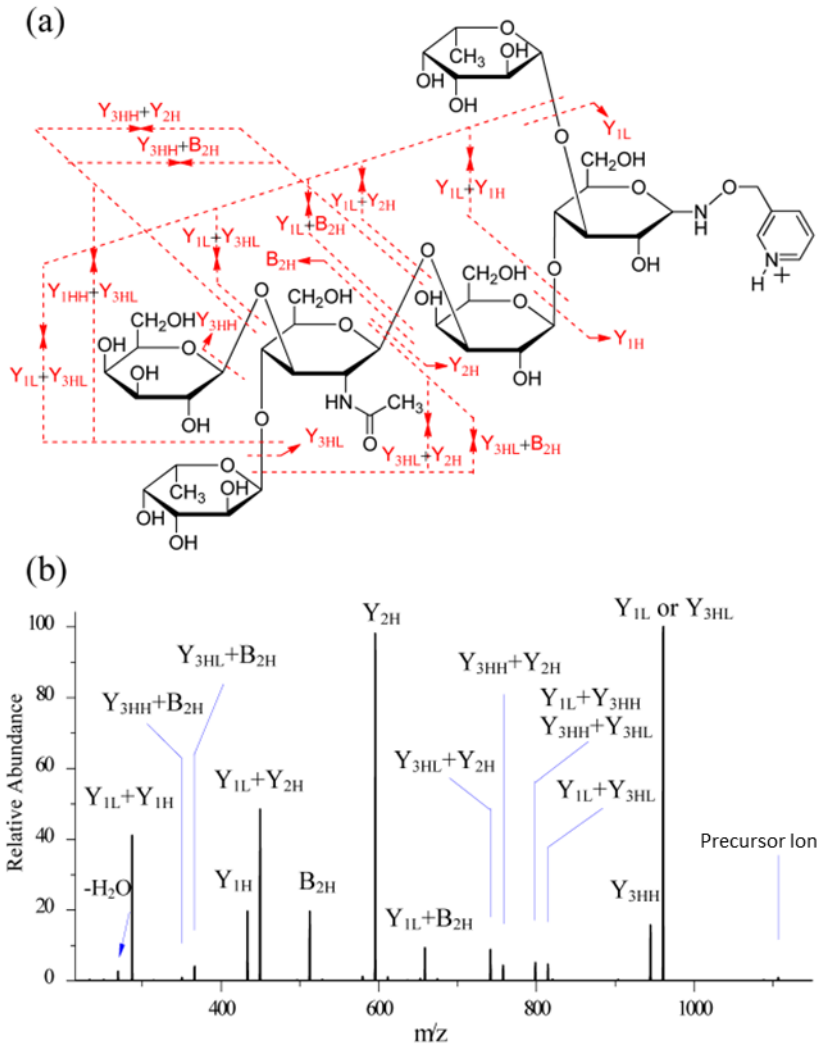

Figure 4. The fragmentation patterns that are observed following the CID of the singly-protonated PRAGS-derivatized LNDFH II (a), and the CID spectrum of the singly-protonated PRAGS-derivatized LNDFH II (b). Precursor ion refers to the protonated molecular ion (Gao *et al.*, 2013).

COMBINATION OF ACID-BASE CHEMISTRY AND FREE RADICAL CHEMISTRY

Recently, free radical chemistry[55] has regained great attention in the field of biomolecular characterization.[56-60] Glycans are also highly susceptible to depolymerization by the free radical processes that are induced via the interactions with reactive oxygen species (ROS) or reactive nitrogen species (RNS).[61] This also agrees with electron-activated dissociation (ExD) techniques for glycan structure analysis, which usually involves fragmentation via the low-energy free radical dissociation pathways. Inspired by the susceptibility of glycans to dissociate by means of free radicals through ExD, a biomimetic free radical activated glycan sequencing (FRAGS) reagent was developed to both understand the reactions between free radicals and glycans and to generate information relevant to the structure of glycans.[54] The FRAGS reagent possesses a free radical precursor for the glycan characterization, a glycan coupling site for covalently attaching glycans by regiospecific derivatization at the reducing terminus, and a mass spectrometric manipulation site for ionization. The FRAGS reagent was demonstrated to generate systematic and predictable cleavages, yielding a wealth of structural information, including the sequence, the linkages, and the branching sites. A series of abundant and systematic dissociation patterns including the Y, ^{0,2}X, ^{1,5}X, Z, and n ions are generated, providing detailed structural information (Figure 3). The systematic Y and Z ions provide composition and sequence information while the ^{0,2}X and n ions provide linkage information. For topological characterization, the ^{1,5}X ions provide useful information. More fragmentation patterns including glycosidic bond cleavage, cross-ring cleavage, IRL, and M-ERL are

observed for LNDFH II, which represents branched glycans (Figure 5). The characteristic Z_{1H}+Z_{1L} provides direct evidence of the two branch structures, such as that found in the FRAGS-derivatized LNDFH II (Figure 5). Starred peaks (Y*) are the product ions corresponding to the glycosidic bond cleavages from the precursor ion without losing TEMPO. Moreover, the Y+Z, and Y+^{1,5}X ions are formed, wherein Y ion results from acid-base chemistry while Z and ^{1,5}X ions result from free radical chemistry.

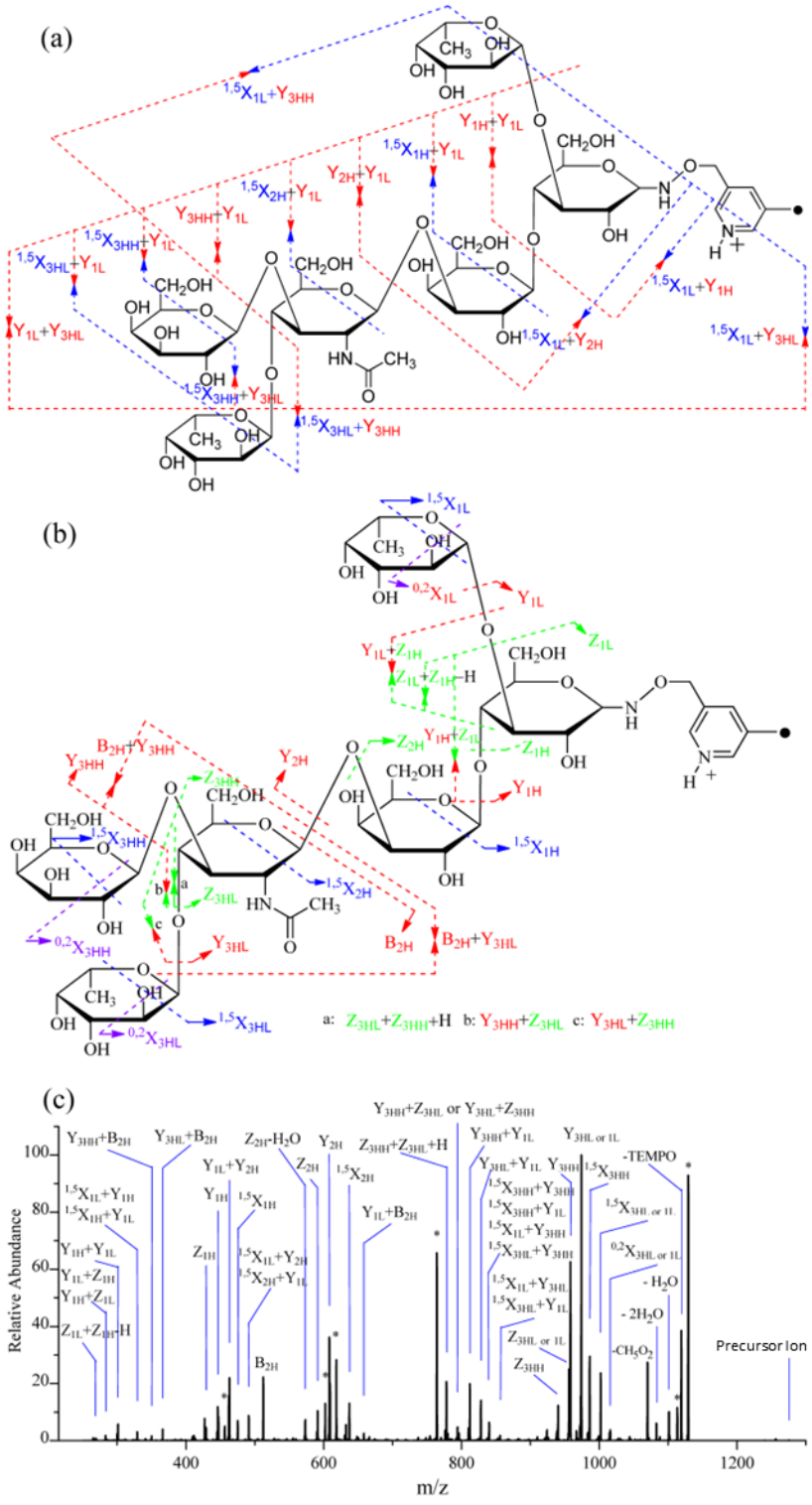

Figure 5. The fragmentation patterns observed following the CID of the singly-protonated FRAGS-derivatized LNDFH II (a and b, two schemes are shown to label all fragmentation patterns in a

deconvoluted manner), and the CID spectrum of the singly-protonated FRAGS-derivatized LNDFH II (c). Starred peaks are the product ions corresponding to the glycosidic bond cleavages from the precursor ion (Gao *et al.*, 2013).

Zhang and Julian reported an alternative way to generate a nascent free radical via the photodissociation of the specific carbon-iodine bond for glycan characterization.[59] The radical precursor is linked to glycans via either covalent reduction amination or noncovalent complexation. The nascent radical, generated by the homolytic bond cleavage of the specific carbon–iodine bonds in protonated systems by either collisional activation or photodissociation, results in the characteristic glycosidic bond cleavage and cross-ring cleavage products. The CID mass spectrum for the singly-protonated maltoheptaose is dominated by fragments resulting from glycosidic bond cleavages (as shown in Figure 6a), with uncertain assignments of the fragments due to the structural symmetry of maltoheptaose. The CID mass spectrum for iodoaniline-derivatized maltoheptaose yields a full series of the Y ions that reveal the nature of each monosaccharide building block. Finally, a close inspection of Figure 6b reveals additional low abundance peaks (shown in greater detail in Figure 6c). These peaks represent the secondary fragments derived from the radical ion. LNDFH I and LNDFH II are two hexasaccharide isomers which differ only in the linkage position of one fucose group (Figure 7). These two isomeric glycans can be differentiated by the generation of a relatively high abundance of the $Z_{4\alpha}$ ion for the LNDFH I isomer and the $Z_{3\alpha\beta}/Z_{1\beta}$ ions for the LNDFH II. Overall, the collisional activation of the radical isomers generates the glycosidic bond cleavage and the cross-ring fragmentations. It needs to be noted that glycan rearrangement ions are also observed due to the mobile proton, similar to the PRAGS and FRAGS reagents.

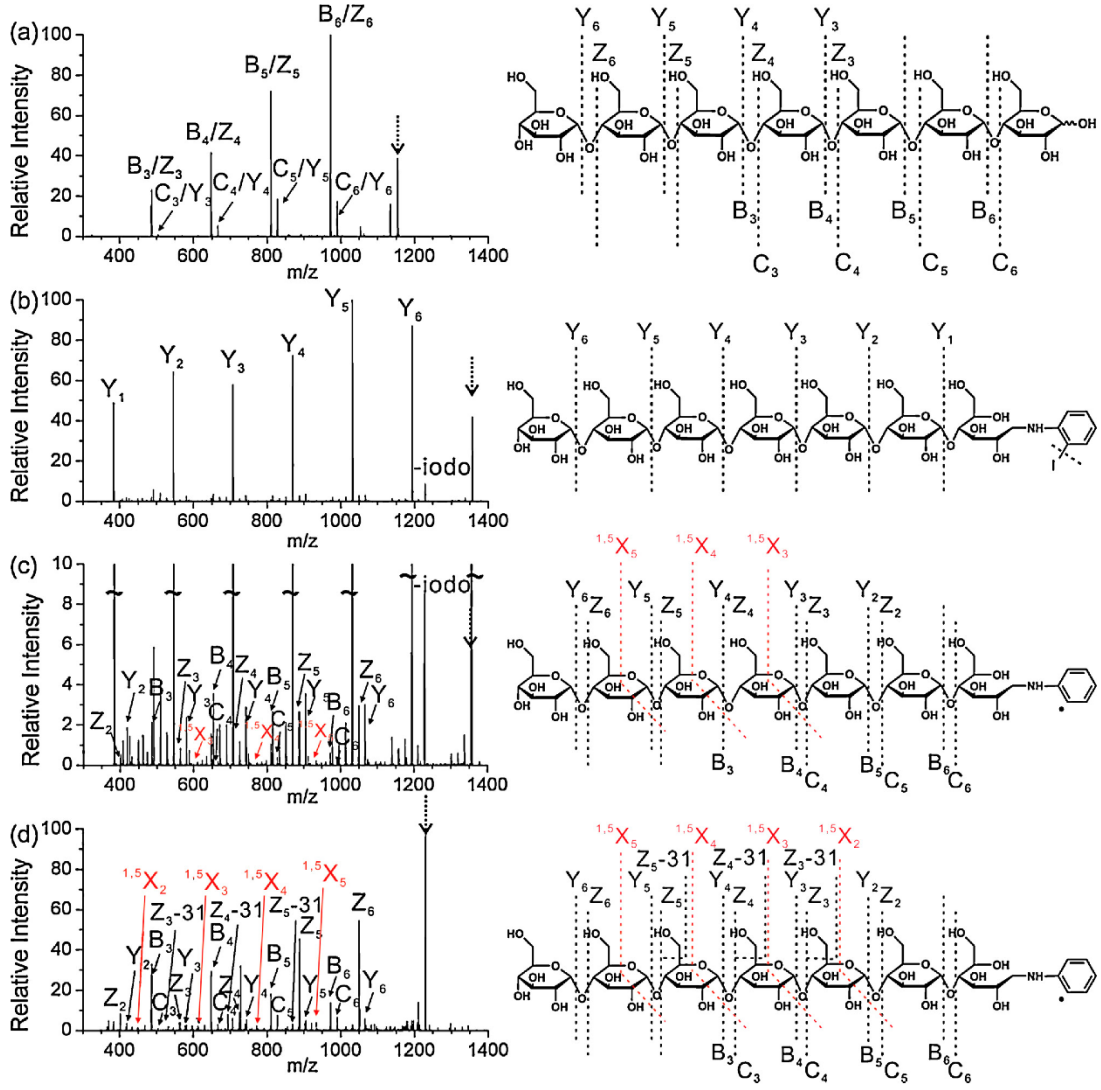

Figure 6. (a) the CID spectrum of the protonated maltoheptaose; the assignments of the peaks are ambiguous due to the maltoheptaose symmetry. (b) the CID spectrum of the protonated maltoheptaose that was previously derivatized with 2-iodoaniline; the X, Y, Z fragments were assigned based on the free radical precursor, which is depicted in the structure shown on the right. (c) the zoomed-in version of Figure 6b. (d) the CID spectrum of the protonated radical maltoheptaose, which was generated by the photodissociation of the 2-iodoaniline-modified maltoheptaose (Zhang *et al.*, 2014).

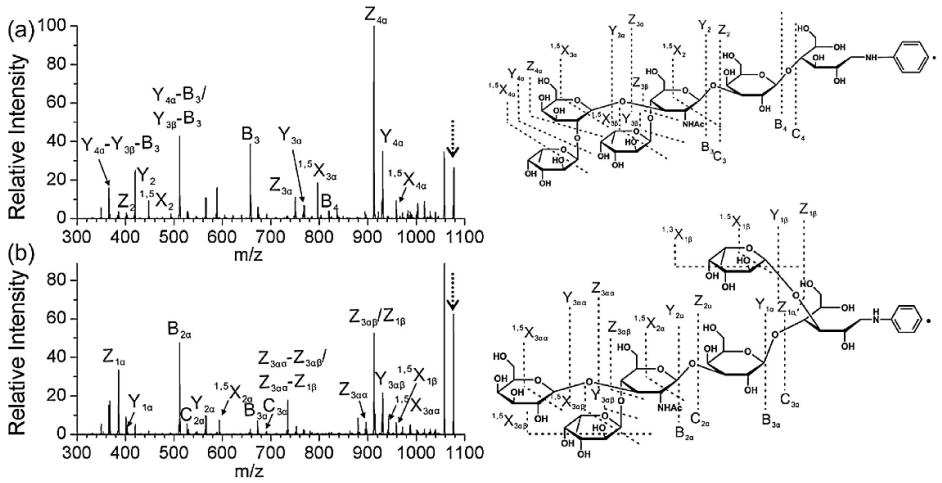

Figure 7. (a) the RDD spectrum of the protonated lacto-N-difucohexaose I (LNDFH I) that was previously modified with 4-iodoaniline. (b) the RDD spectrum of the protonated LNDFH II isomer that was previously modified with 4-iodoaniline (Zhang *et al.*, 2014).

FREE RADICAL CHEMISTRY

As briefly mentioned, the unpredictable gas-phase glycan rearrangements mislead the structural analysis. For instance, the fucose migration is the most common rearrangement observed upon the activation of the gas-phase glycan ions and yet is unpredictable.[62-64] Fucose mostly exists as a terminal modification of oligosaccharides that are not further elongated, which is involved in a wide variety of biological and pathological processes, and is one of the most common and important types of glycosylation in cancer and inflammation.[65-67] It is therefore of great importance to avoid the mass spectrometric fucose migration to obtain accurate glycan structures. Although different mechanisms have been proposed for fucose migration, the labile proton plays a pivotal role in the proposed dissociation pathways.[62,64,68] To address this problem, Beauchamp and Gao et al. designed and synthesized the methylated free radical activated glycan sequencing reagent (Me-FRAGS, Figure 2), which contains a free radical precursor and a fixed charge on a pyridine moiety.[69] Like the PRAGS and FRAGS reagents described previously,[54,70] the Me-FRAGS reagent reacts selectively with the aldehyde and keto groups and thus targets glycans with regiospecific derivatization at the reducing terminus. Three pairs of glycan isomers, differing only in the location of the fucose subunit in each pair, are employed here to test the capability of the Me-FRAGS reagent.

The 2'-fucosyllactose and 3-fucosyllactose differ only in the location of a single fucose subunit. The fucose subunit is bonded to the galactose subunit of lactose through an α1-2 linkage in 2'-fucosyllactose but to the glucose subunit of lactose via an α1-3 linkage in 3-fucosyllactose (Figure 8). As controls, the CID spectra of the PRAGS- and FRAGS-derivatized 2'-fucosyllactose and 3-fucosyllactose ions are discussed. The Y ions, internal residue loss (IRL) ions, and multiple external residue losses (M-ERL) ions were observed in the CID spectra of the PRAGS-derivatized 2'-fucosyllactose and 3-fucosyllactose (Figure 8). The Y_1+Y_2 (IRL) ion formed by the fucose migration of the 2'-fucosyllactose has the same mass as the product ion $Y_{1\alpha}$ of the 3-fucosyllactose. Moreover, the $Y_{1\alpha}$+$Y_{1\beta}$ (M-ERL) ion for the 3-fucosyllactose has the same mass as the Y_1 ion for the 2'-fucosyllactose. The IRL and M-ERL jointly contribute to the generation of two similar CID spectra, making the differentiation of these two simple

glycan isomers and the unknown glycan analysis difficult and ambiguous. More extensive fragmentation, including the glycosidic bond cleavage (Y and Z), and the cross-ring cleavage (^{1,5}X and ^{0,2}X) are generated when employing the FRAGS reagent (Figure 8). Product ions that were formed via IRL and M-ERL are also observed, such as the Y_1+Y_2 and the $Y_{1\alpha}$+$Y_{1\beta}$ ions (Figure 8). Moreover, the Y* ions are generated via the glycosidic bond cleavage directly from the precursor ion with the retention of the radical precursor. The labile proton is proposed to be the origin of the IRL, M-ERL, and Y* ions. Furthermore, the Y+Z and Y+^{1,5}X ions are generated by the combination of acid-base and free radical chemistry, wherein the Y ion originates from the fragmentation generated by the labile proton while the Z and ^{1,5}X ions result from the free radical. The generation of the IRL, M-ERL, Y*, Y+Z, and Y+^{1,5}X ions increases the complexity of the spectra, making the interpretation of glycan structure and differentiation of these isomeric glycans ambiguous. Me-FRAGS reagent was developed to eliminate the formation of the labile proton and thus eradicate the potential for glycan rearrangements. As expected, the disappearance of the IRL, M-ERL, Y*, Y+Z, and Y+^{1,5}X ions significantly decreased the complexity of the MS^2 spectra (Figure 8). Fortunately, all of the essential Y– and Z–type glycosidic bond, ^{1,5}X cross-ring, and Z_α+Z_β cleavages are preserved for the characterization of glycans. The Z_α+Z_β ion serves as a diagnostic product ion that identifies the type of branching structure. The resulting systematic free radical directed dissociation of the glycan inspired the development of a radical-driven glycan deconstruction diagram (R-DECON diagram), which visually summarizes the MS^2 results and thus allows for the assembly of the glycan skeleton (Figure 9). Clearly, the branch site can also be identified by the Y, Z, and ^{1,5}X ions (Figure 9) in the glycan R-DECON diagrams. Therefore, the 2'-fucosyllactose and 3-fucosyllactose can be differentiated unambiguously by Me-FRAGS by means of preserving the radical chemistry but eliminating the acid-base chemistry. To further assess the capability of the Me-FRAGS reagent to distinguish more complex isobaric, yet branched, glycan structures, LNFP I and V, and LNDFH I and II were examined. Each pair of glycan isomers differ only in the location of one fucose subunit but can be easily distinguished by the unique fragmentation patterns. Again, the Z, Y (Y_M and Y_{M+2}), ^{1,5}X, and Z_α+Z_β ions are generated (Figure 10) and the R-DECON diagram facilitates the straightforward visualization of the glycan skeleton (Figure 11). The branch sites can be confirmed unambiguously by the Z_α+Z_β ions ($Z_{1\alpha}$+$Z_{1\beta}$ for LNDFH I, $Z_{1\alpha}$+$Z_{1\beta}$ and $Z_{3\alpha\alpha}$+$Z_{3\alpha\beta}$ for LNDFH II). Moreover, the relative abundance of the Z_α+Z_β ion increases greatly by eliminating the acid-base chemistry, which supports the radical-driven mechanism for forming this ion proposed previously.[54]

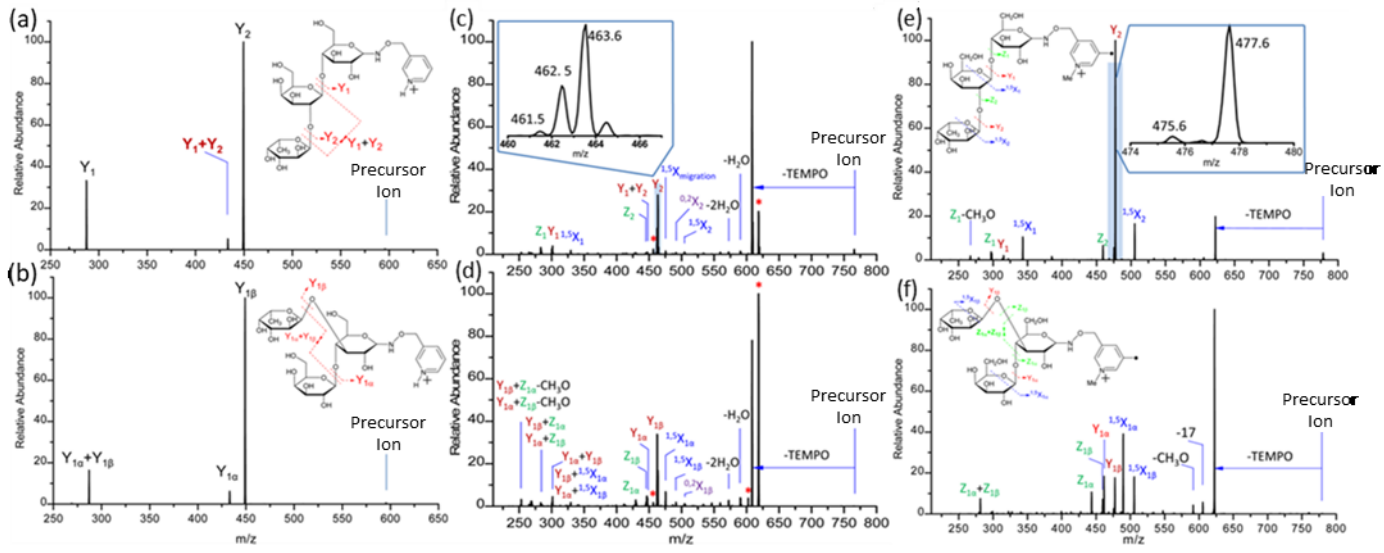

Figure 8. The CID spectra of the singly-protonated PRAGS-derivatized 2'-fucosyllactose (a) and 3-fucosyllactose (b), and the fragmentation patterns observed following the CID of the singly-protonated PRAGS-derivatized 2'-fucosyllactose and 3-fucosyllactose, respectively. The parent ion refers to the protonated molecular ion. The CID spectra of the singly-protonated FRAGS-derivatized 2'-fucosyllactose (c) and 3-fucosyllactose (d). The parent ion refers to the protonated molecular ion. The peaks that are

marked with asterisks are the product ions which correspond to the glycosidic bond cleavages from the precurspr ion. The fragmentation patterns observed following the CID of the Me-FRAGS-derivatized 2'-fucosyllactose (e) and 3-fucosyllactose (f), and the CID spectra of the Me-FRAGS-derivatized 2'-fucosyllactose and 3-fucosyllactose, respectively. The precursor ion refers to the methylated molecular ion (Desai *et al.*, 2016).

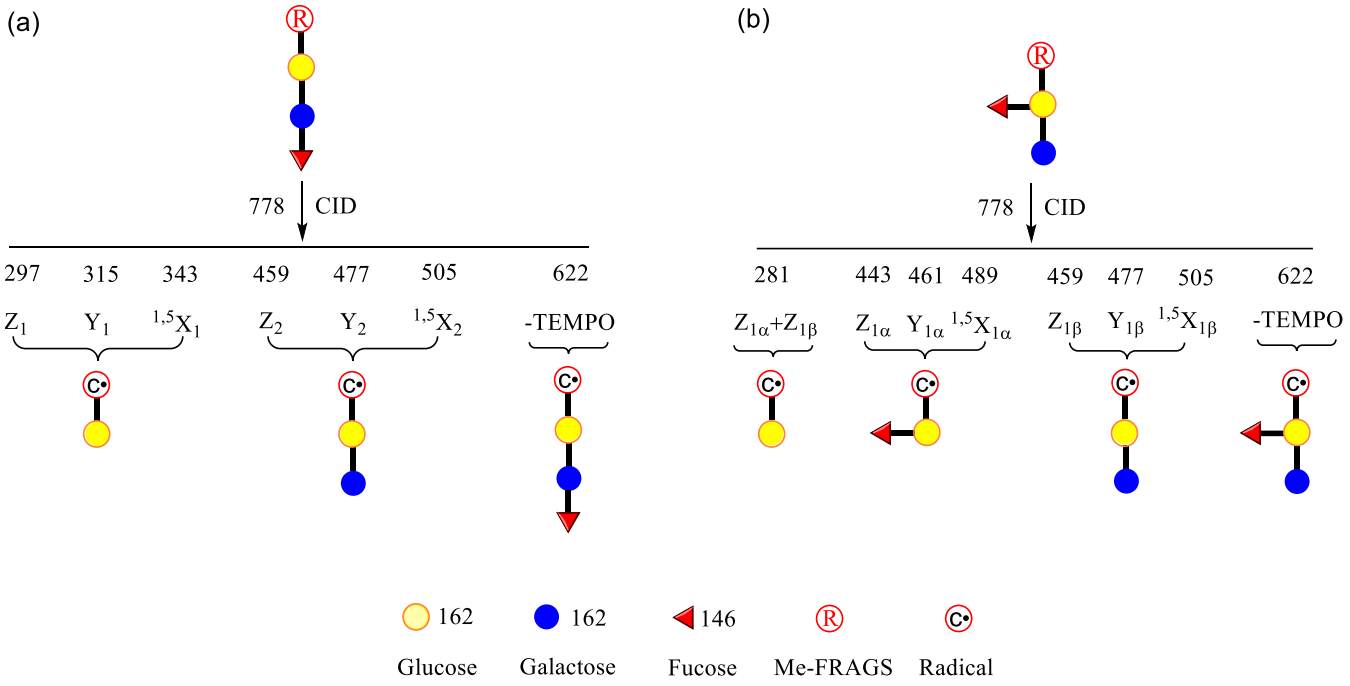

Figure 9. The glycan R-DECON diagrams for the Me-FRAGS derivatized 2'-FL (a) and 3-FL (b). The precursor ion (m/z 778) is subjected to MS^2 to generate a series of ions with m/z values from 281 to 622 (Desai *et al.*, 2016).

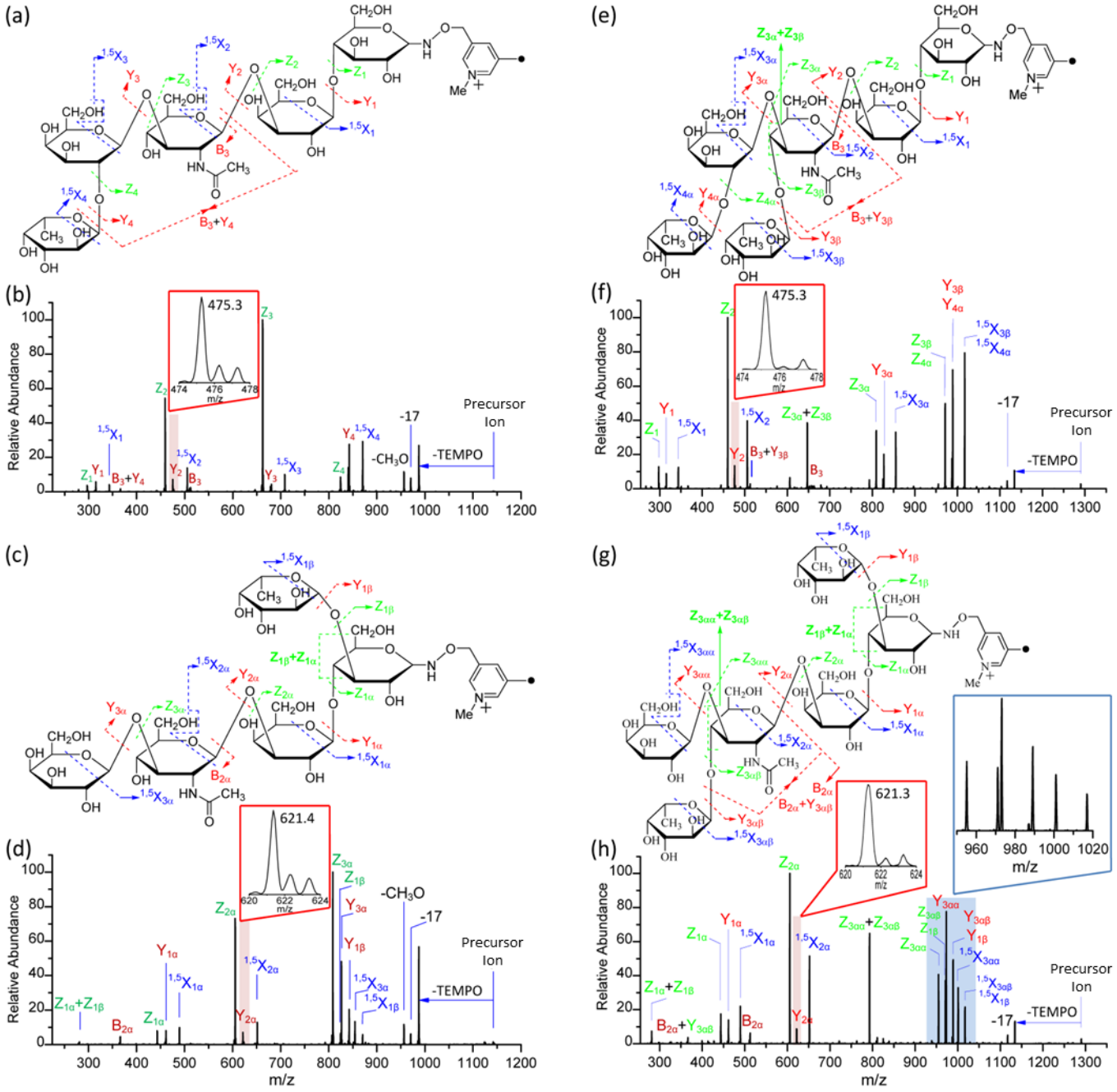

Figure 10. The fragmentation patterns observed following the CID of Me-FRAGS-derivatized LNFP I (a), LNFP V (c), LNDFH I (e), and LNDFH II (g), and the CID spectra of the Me-FRAGS-derivatized LNFP I (b), LNFP V (d), LNDFH I (f), and LNDFH II (h). The precursor ion refers to the methylated molecular ion (Desai *et al.*, 2016).

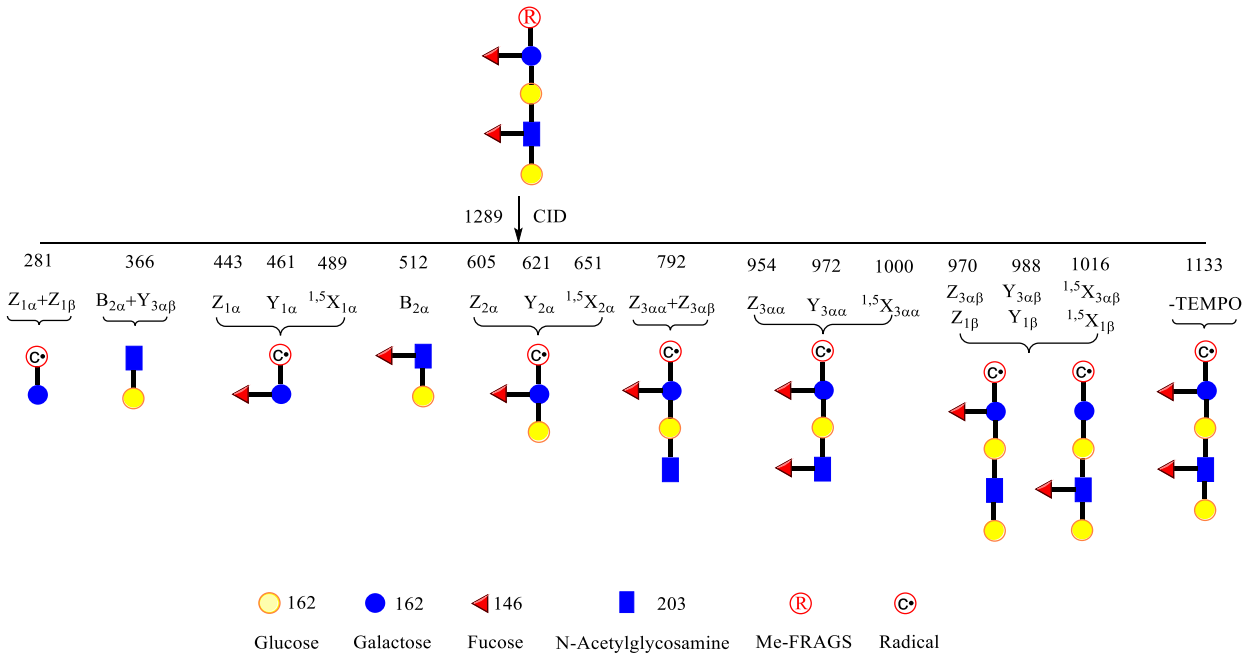

Figure 11. The glycan radical R-DECON diagram for the Me-FRAGS derivatized LNDFH II. The precursor ion (m/z 1289) is subjected to MS^2 to generate a series of ions with m/z values from 281 to 1133 (Desai *et al.*, 2016).

GLYCAN ISOMER DIFFERENTIATION

Combined with Orbitrap HCD and ion trap CID, Me-FRAGS has been used to differentiate glycan anomers, epimers, and constitutional isomers via simple one-step collisional activation, which generates unique precursor-structure-dependent fragment ions and/or fragment ions with different relative intensities.[71] The fragmentation patterns and relative abundances of fragment ions upon the ion trap CID of the Me-FRAGS-derivatized nigerose are independent of the collision energy due to the slow heating process (Figure 12). In contrast, both the fragmentation patterns and the relative abundances of the fragment ions of the Me-FRAGS-derivatized nigerose are dependent upon the Orbitrap HCD collisional energy. As a result, more fragmentation patterns are generated from Orbitrap HCD than ion trap CID. The relative abundance of the ion corresponding to the loss of TEMPO increases as the Orbitrap HCD collisional energy is increased from 15 to 25 but decreases dramatically once the Orbitrap HCD collisional energy is increased beyond 35 (Figure 12). Meanwhile, the relative abundance of the low-mass fragment ions increases significantly as the Orbitrap HCD collisional energy is ramped up. For instance, the relative abundances of the Z_1-H_2O ion (*m/z* 279), Y_1+2H ion (*m/z* 315), Z_1-$C_3H_6O_3$ ion (*m/z* 223), and $^{1,5}X_0$+H ion (*m/z* 181) increase significantly. Moreover, new fragment ions are generated at high Orbitrap HCD collisional energy, such as the $^{1,4}X_0$-CH_2O• ion (*m/z* 193) and the $^{1,4}X_0$-OH• ion (*m/z* 207). As a result, the Orbitrap HCD of the Me-FRAGS derivatized nigerose generates diverse, yet informative, fragment ions, which could be used as a "fingerprint" to determine the glycan linkages, anomeric center configuration, and stereocenters. The Y_1-$C_2H_4O_2$ ion (*m/z* 253) is characteristic for 1-4 linkage disaccharides, such as maltose, cellobiose, and lactose (Figure 13). Moreover, the Y_1+H-CH_2O (*m/z* 284) ion is unique for 1-6 linkage disaccharides, such as isomaltose, gentiobiose, and melibiose (Figure 13), which is further confirmed by the study of the Me-FRAGS-derivatized glucose tetrasaccharide with one

terminal α-1→6 linkage. The disaccharide isomers with the same linkage site have similar Orbitrap HCD spectra but can be differentiated by R_{isomer} values, which are calculated by using the following equation wherein R_1 and R_2 refer to the abundance ratios of the two selected pairs of MS^n fragment ions.

$$R_{\text{isomer}} = \frac{R_1}{R_2}$$

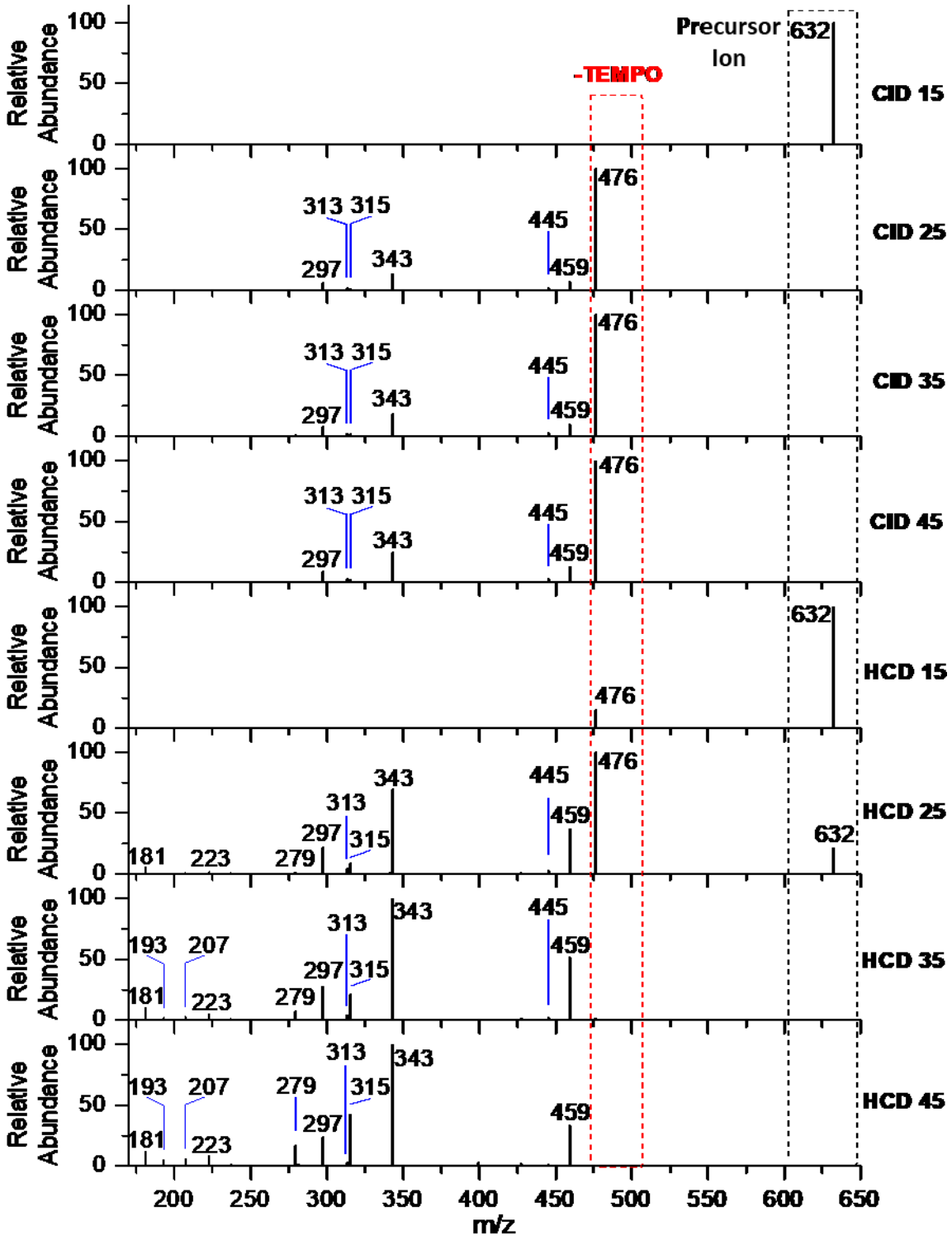

Figure 12. The MS^2 spectra of the Me-FRAGS derivatized nigerose by CID and HCD with collisional energies of 15, 25, 35, and 45 (Murtada *et al.*, 2020).

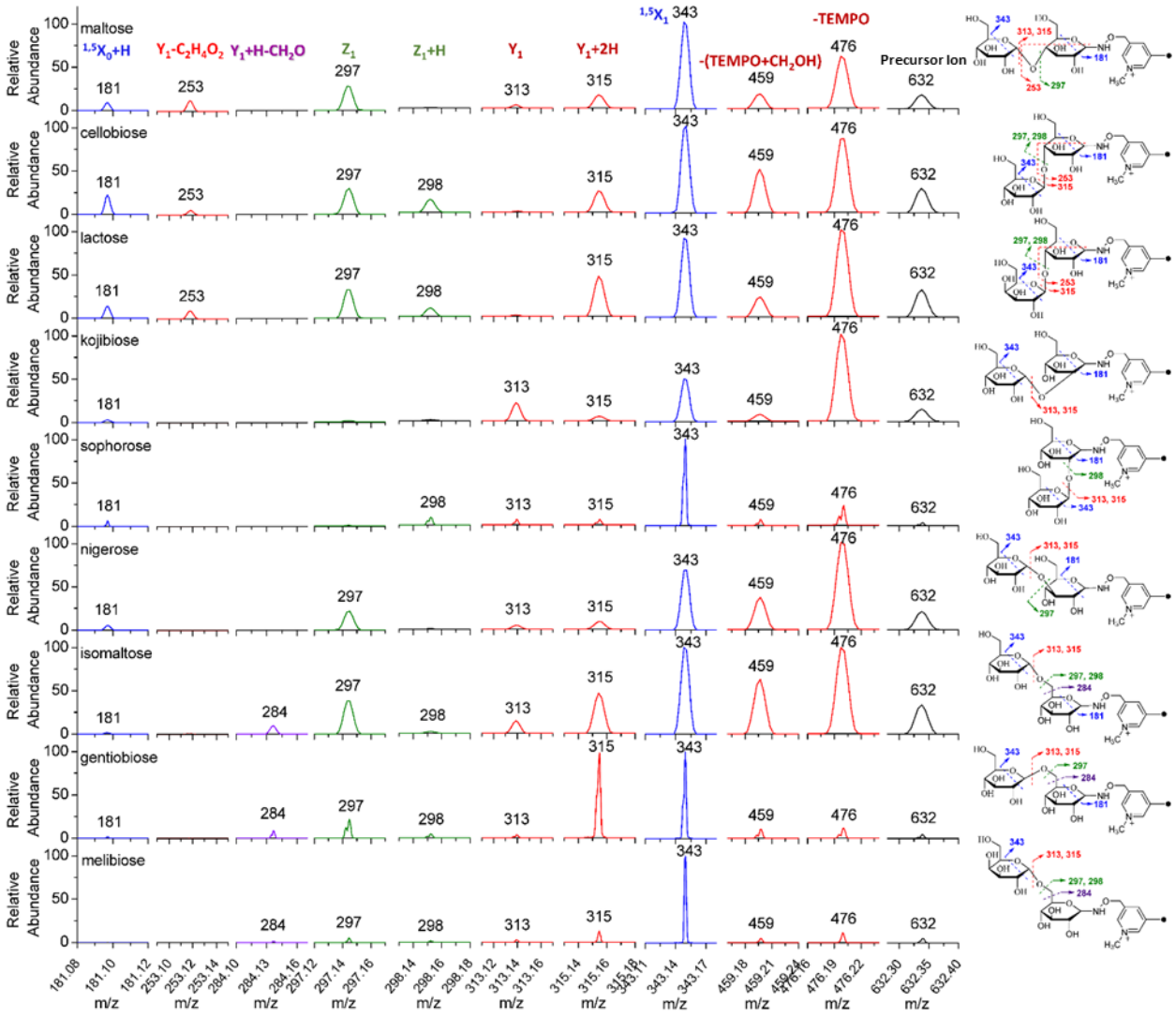

Figure 13. The zoomed in MS^2 spectra of the Me-FRAGS derivatized disaccharides that were subjected to HCD with a collisional energy of 25 (Murtada *et al.*, 2020).

The mass spectrometric analysis of glycans has been hampered by trace amounts of glycan sample available from low-abundant glycoconjugates in biological sources. It is therefore especially challenging to directly analyze glycans by MS with even traces of these other components as some species, including proteins and peptides, are often much more readily ionized, and thereby greatly suppress glycan ionization and detection. As a result, efficient glycan enrichment and separation from complex biological mixtures are crucial for mass spectrometric glycan characterization. To address these issues, a multi-functional solid-supported free radical probe (SS-FRAGS, Scheme 1) was developed by Gao and Beauchamp.[72] The probe comprises a solid support, disulfide bond, free radical precursor, pyridyl, and hydrazine moieties. SS-FRAGS selectively captures free glycans, allowing for their enrichment and purification. The disulfide bond acts as a temporary covalent linkage between the solid support and the free radical reagent, allowing the release of glycans via the cleavage of this bond after enrichment and purification. The free radical precursor generates a nascent free radical upon collisional activation, which simultaneously initiates low-energy free radical dissociation pathways, thus,

fragmenting the glycan. The pyridyl functional group allows for a fixed charge, thereby allowing for glycan structure determination from the analysis of the systematic fragmentation of the glycan back towards the reducing terminus without the potential for glycan rearrangements. The hydrazide functional group selectively targets bioconjugates at the reducing terminus of the glycan, thereby serving as a coupling site between the reagent and the glycan.

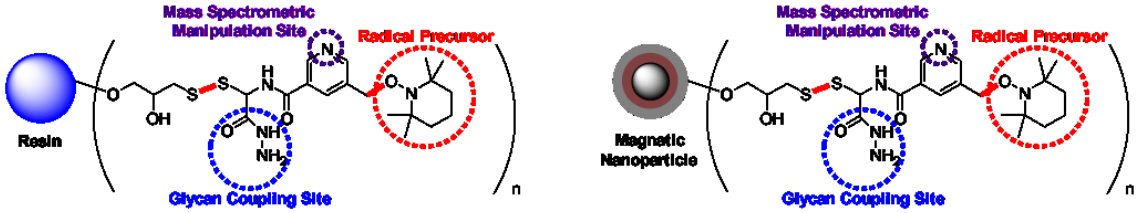

Scheme 1. The structures of the solid-supported free radical probes.

GLYCAN ENRICHMENT AND CHARACTERIZATION

Glycans are selectively captured through covalent conjugation to the SS-FRAGS via the reduction reaction between the unique glycan reducing terminus and the probe hydrazide moiety (glycan coupling site of the probe, Figure 14). To achieve glycan purification and enrichment, the impurities and/or excess reactants are thoroughly washed away by water and acetonitrile. After enrichment, the conjugated glycans are released by the selective cleavage of the disulfide bond by using the chemical scissors, dithiothreitol (DTT). Then, the conjugated glycans are methylated by reacting with iodomethane at the pyridine nitrogen site to avoid glycan rearrangement during collisional activation, ionized by electrospray ionization (ESI), and subjected to collision-induced dissociation (CID) within the ion trap. LNDFH I and II were employed as branched isobaric glycans to assess the capability of the SS-FRAGS to analyze more complicated glycan structures and differentiate glycan isomers. Similarly, systematic and predictable radical-directed glycan fragment ions are generated upon collisional activation, including Z, Y, ^{1,5}X, and Z_α+Z_β ions retaining the charge on the reducing terminus. More importantly, the unique fragmentation pattern Z_α+Z_β ($Z_{3\alpha}$+$Z_{3\beta}$ for LNDFH I and $Z_{1\alpha}$+$Z_{1\beta}$ and $Z_{3\alpha\alpha}$+$Z_{3\alpha\beta}$ for LNDFH II, Figure 15) is observed only at the branch site, providing the information to confirm the presence and location of the branch structure. It is essential to note that the two glycosidic linkages need to be adjacent to each other to observe the unique Z_α+Z_β ion. The glycan LNDFH I has β1-3 and α1-4 linkages on the branch site while LNDFH II has α1-3 and β1-4 linkages on the first branch site and β1-3 and α1-4 linkages on the second branch site. The determination of the branch sites with two glycosidic linkages which are not adjacent to each other will be discussed in the case of glycans released from RNase B (*vide infra*).

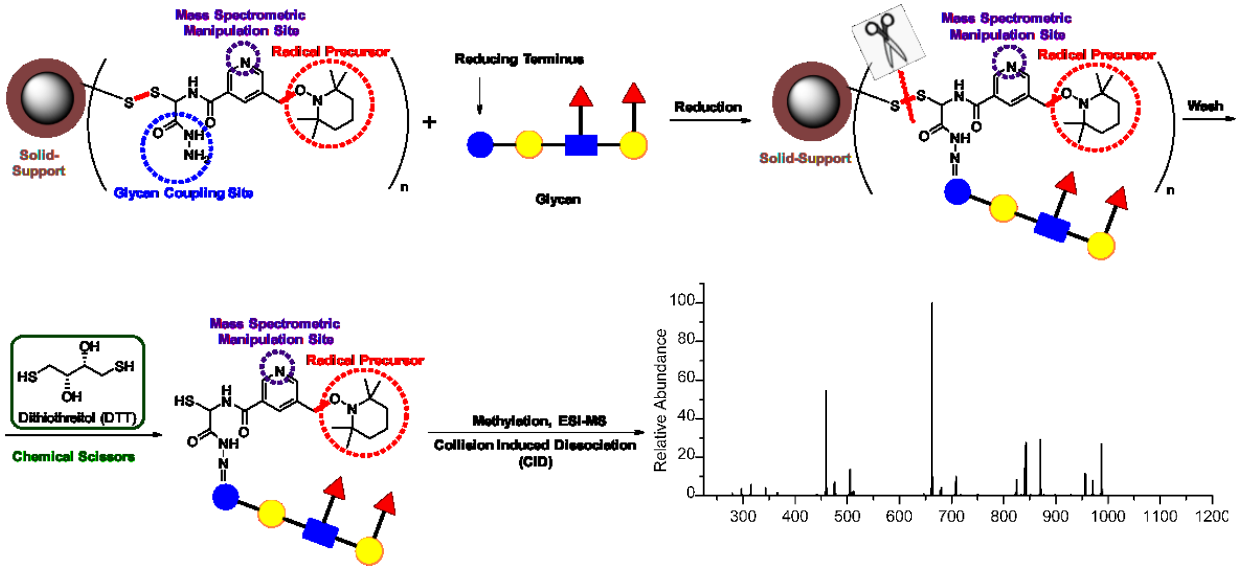

Figure 14. A schematic diagram of glycan capture, release, and MS analysis (Fabijanczuk *et al.*, 2019).

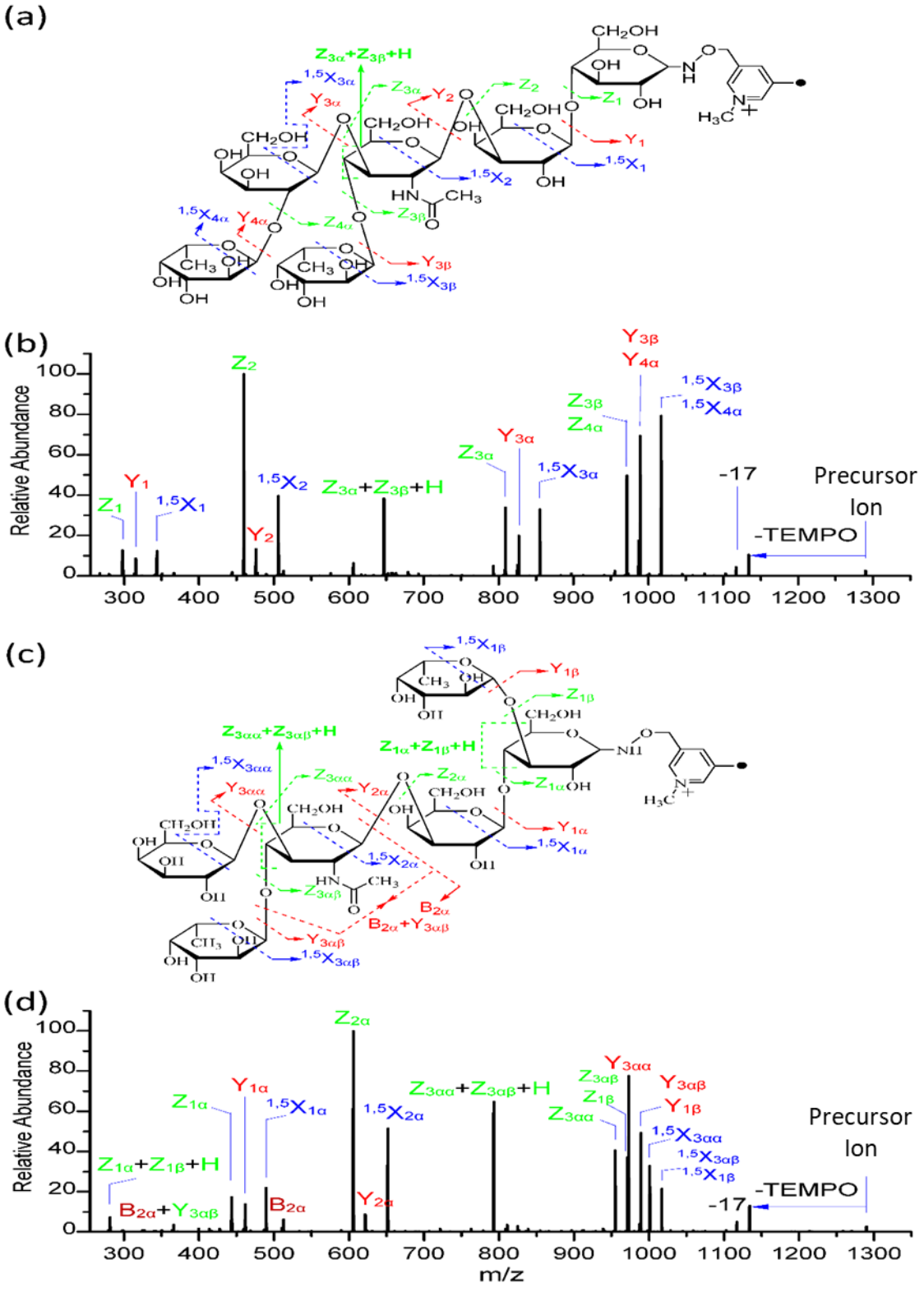

Figure 15. The fragmentation patterns observed following the MS^2 CID of the MNPs-FRAGS-derivatized LNDFH I (a), LNDFH II (c), and the CID spectra of the MNPs-FRP-derivatized LNDFH I (b), LNDFH II (d) (Fabijanczuk *et al.*, 2019).

To test the capability of the SS-FRAGS for the enrichment of glycans from biological samples, the analysis of glycans released from ribonuclease B (RNase B) from bovine pancreas was performed. The RNase B (1 mg) was denatured at 90 °C for one hour. Then, the glycans were enzymatically released from the RNase B by PNGase F followed by the enrichment protocol described in Figure 14. Although PNGase F is the most common route for glycan liberation, those through chemical means are still well-established. Recently, sodium hypochlorite (the active ingredient in commercial bleach) has shown the capability to release free reducing glycans from glycoproteins.[73] Either way, after glycan release prior to utilizing the SS-FRAGS and following the procedure described in Figure 14, all of the impurities, including the proteins, peptides, salts, and detergents, were easily washed away by water and acetonitrile, allowing for the purification and enrichment of glycans. Using SS-FRAGS is advantageous relative to the derivatization of glycans with other previously described reagents in that it requires less effort and time for enrichment by utilizing a solid-support. As shown in Figure 16, abundant ions were detected, enabling subsequent collision-induced dissociation for further structural characterization of the glycans released from the RNase B, which is further discussed below. The FRAGS reagent (Figure 16b), which was proved to allow for the systematic and predictable cleavages for glycan structure elucidation, was used as a point of comparison to provide support for the capability of the solid-supported probe for enriching glycans. Ultimately, no signal was observed for the parallel control test (Figure 16b). To further compare the SS-FRAGS with C_{18} solid-phase extraction (SPE), the SPE purification was run after the derivatization of FRAGS. Either way, it is clear that the SS-FRAGS obtains better glycan purification than SPE.

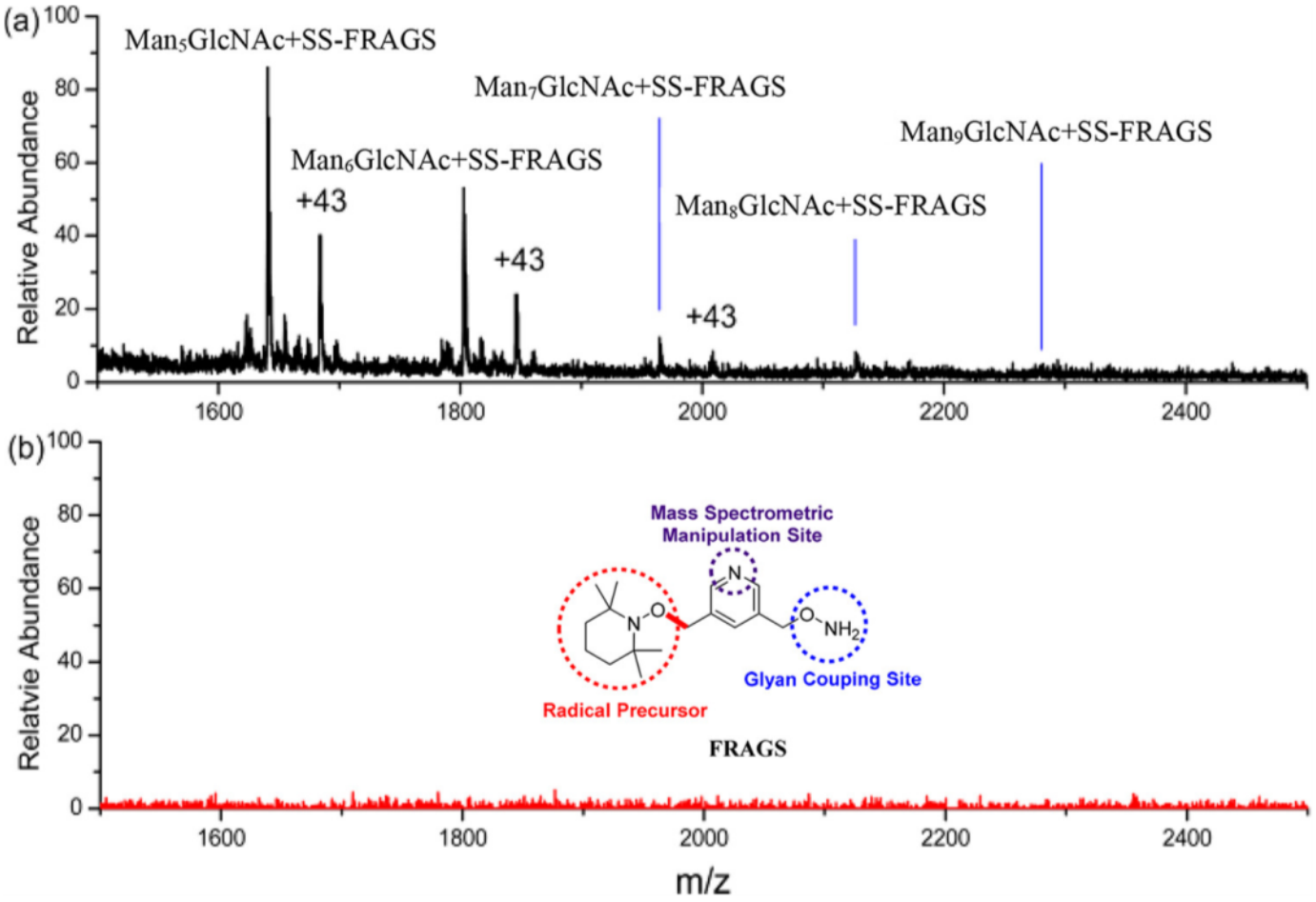

Figure 16. The enrichment of glycans released from RNase B by the SS-FRAGS (a), and the control by using the FRAGS reagent (b) (Fabijanczuk *et al.*, 2019).

As previously mentioned, abundant mass spectrometric signals were observed for the target glycans that were released from RNase B. Figure 17 shows the CID mass spectra of the free radical probe-derivatized glycans that were released from RNase B. As expected, only the systematic Z, Y, and ^{1,5}X cleavages were generated due to the presence of the well-defined site of radical generation.. For the glycans released from RNase B, the structure of the most abundant isomer of $Man_5GlcNAc_2$ is proposed and validated to have two branch sites with distal glycosidic linkages. The configuration of these two branch sites is confirmed by the corresponding loss of mannose subunits on each side of the branch site. Furthermore, there is an absence of fragmentations that would otherwise pertain to the loss of two mannose or four mannose residues for $Man_5GlcNAc_2$.

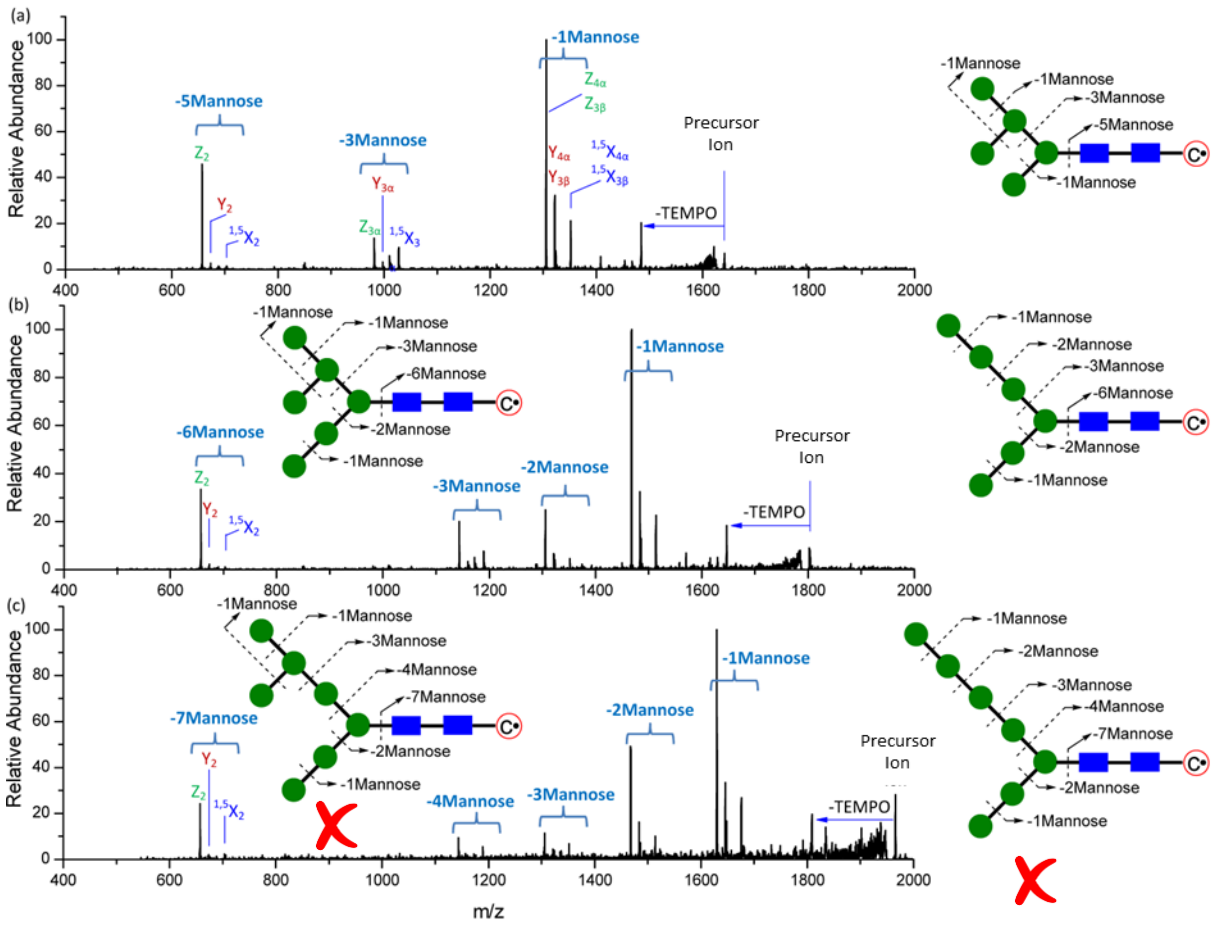

Figure 17. The fragmentation patterns observed following the CID of the MNPs-FRP-derivatized $Man_5GlcNAc_2$ (a), $Man_6GlcNAc_2$ (b), and $Man_7GlcNAc_2$ (c). The precursor ion refers to the methylated molecular ion (Fabijanczuk *et al.*, 2019).

CONCLUSIONS AND PERSPECTIVES

The development of reagents recruiting acid-base and/or free-radical chemistry has shown the ability to accurately characterize glycans based on the induction of unique product ions. Acid-base chemistry excels at dissociating glycans into their constituent components at glycosidic bonds. However, the unpredictable glycan rearrangement ions can mislead the interpretation of MS^2 spectra. Fortunately, free radical chemistry with the development of a fixed charge eradicates all of the IRL, M-ERL, Y*, Y+Z, and Y+^{1,5}X ions while retaining all of the essential Y– and Z–type glycosidic bond, ^{1,5}X cross-ring, and Z_α+Z_β cleavages. Additionally, reagents that make use of radical chemistry brings the power of the election dissociation techniques without the need for additional instrumentation. Currently, the aforementioned reagents are capable of accurately distinguishing among branched isobaric isomers similar to lacto-*N*-difucohexaose I and II and branched *N*-glycans that were liberated from glycoproteins similar to RNase B. Such capabilities could translate into the future characterization of human disease glycan biomarkers or quality assurance assays of glycosylated biopharamceuticals.

However, given that these reagents are limited to glycan characterization, the future development of fluorescent free-radical tags for simultaneous glycan quantitation and characterization would

be desirable for the field of glycomics. For example, abnormal quantities of certain human disease glycan biomarkers can be just as essential to monitor as the structure of glycosylations. Thus, the implementation of a sensitive and quantitative analytical technique of glycans with simultaneous characterization capabilities is ideal for the comprehensive study of glycans. For the biopharmaceutical industry, it is just as important to monitor the amount of glycosylations on biologics as part of a more extensive quality assurance assay. For instance, slight differences in the number of glycosylations can significantly impact the safety and efficacy of glycosylated biopharmaceuticals. Thus, in the future, the development of a reagent that is capable of both glycan quantitation via fluorescence and glycan characterization via free radical-mediated processes is an attractive and impactful project to pursue next.

ACKNOWLEDGMENTS

This study was supported by the National Science Foundation through grant CHEM 2107798, MRI 2116596, CHEM1709272, and the National Institutes of Health through grant 1R15GM121986-01A1.

REFERENCES

1. Dove A. The bittersweet promise of glycobiology. *Nature Biotechnology.* 2001;19(10):913-917.
2. Ohtsubo K, Marth JD. Glycosylation in cellular mechanisms of health and disease. *Cell.* 2006;126(5):855-867.
3. Pinho SS, Reis CA. Glycosylation in cancer: mechanisms and clinical implications. *Nature Reviews Cancer.* 2015;15(9):540-555.
4. Taniguchi N, Kizuka Y. Glycans and cancer: role of N-glycans in cancer biomarker, progression and metastasis, and therapeutics. *Adv Cancer Res.* 2015;126:11-51.
5. Freeze HH. Understanding human glycosylation disorders: biochemistry leads the charge. *J Biol Chem.* 2013;288(10):6936-6945.
6. Magalhaes A, Ismail MN, Reis CA. Sweet receptors mediate the adhesion of the gastric pathogen Helicobacter pylori: glycoproteomic strategies. *Expert Rev Proteomic.* 2010;7(3):307-310.
7. Frenkel-Pinter M, Shmueli MD, Raz C, et al. Interplay between protein glycosylation pathways in Alzheimer's disease. *Sci Adv.* 2017;3(9):e1601576.
8. Townsend RR, Hardy MR, Hindsgaul O, Lee YC. High-performance anion-exchange chromatography of oligosaccharides using pellicular resins and pulsed amperometric detection. *Anal Biochem.* 1988;174(2):459-470.
9. Jin C, Harvey DJ, Struwe WB, Karlsson NG. Separation of Isomeric O-Glycans by Ion Mobility and Liquid Chromatography-Mass Spectrometry. *Anal Chem.* 2019;91(16):10604-10613.
10. Wei J, Tang Y, Bai Y, et al. Toward Automatic and Comprehensive Glycan Characterization by Online PGC-LC-EED MS/MS. *Anal Chem.* 2020;92(1):782-791.
11. Hoffstetter-Kuhn S, Paulus A, Gassmann E, Widmer HM. Influence of borate complexation on the electrophoretic behavior of carbohydrates in capillary electrophoresis. *Anal Chem.* 1991;63:1541-1547.
12. Szabo Z, Guttman A, Rejtar T, Karger BL. Improved sample preparation method for glycan analysis of glycoproteins by CE-LIF and CE-MS. *Electrophoresis.* 2010;31(8):1389-1395.

13. Harvey DJ, Scarff CA, Crispin M, Scanlan CN, Bonomelli C, Scrivens JH. MALDI-MS/MS with Traveling Wave Ion Mobility for the Structural Analysis of N-Linked Glycans. *J Am Soc Mass Spectr.* 2012;23(11):1955-1966.
14. Huang YT, Dodds ED. Discrimination of Isomeric Carbohydrates as the Electron Transfer Products of Group II Cation Adducts by Ion Mobility Spectrometry and Tandem Mass Spectrometry. *Analytical Chemistry.* 2015;87(11):5664-5668.
15. Hofmann J, Hahm HS, Seeberger PH, Pagel K. Identification of carbohydrate anomers using ion mobility-mass spectrometry. *Nature.* 2015;526(7572):241-244.
16. Warnke S, Ben Faleh A, Scutelnic V, Rizzo TR. Separation and Identification of Glycan Anomers Using Ultrahigh-Resolution Ion-Mobility Spectrometry and Cryogenic Ion Spectroscopy. *J Am Soc Mass Spectrom.* 2019;30(11):2204-2211.
17. Ben Faleh A, Warnke S, Rizzo TR. Combining Ultrahigh-Resolution Ion-Mobility Spectrometry with Cryogenic Infrared Spectroscopy for the Analysis of Glycan Mixtures. *Anal Chem.* 2019;91(7):4876-4882.
18. Fu D, Chen L, O'Neill RA. A detailed structural characterization of ribonuclease B oligosaccharides by 1H NMR spectroscopy and mass spectrometry. *Carbohydr Res.* 1994;261(2):173-186.
19. Szymanski CM, Michael FS, Jarrell HC, et al. Detection of conserved N-linked glycans and phase-variable lipooligosaccharides and capsules from campylobacter cells by mass spectrometry and high resolution magic angle spinning NMR spectroscopy. *J Biol Chem.* 2003;278(27):24509-24520.
20. Harvey DJ. Ionization and collision-induced fragmentation of N-linked and related carbohydrates using divalent canons. *Journal of the American Society for Mass Spectrometry.* 2001;12(8):926-937.
21. Adamson JT, Hakansson K. Electron capture dissociation of oligosaccharides ionized with alkali, alkaline earth, and transition metals. *Analytical Chemistry.* 2007;79(7):2901-2910.
22. Konda C, Bendiak B, Xia Y. Linkage determination of linear oligosaccharides by MS(n) (n > 2) collision-induced dissociation of Z(1) ions in the negative ion mode. *J Am Soc Mass Spectrom.* 2014;25(2):248-257.
23. Pellegrinelli RP, Yue L, Carrascosa E, Warnke S, Ben Faleh A, Rizzo TR. How General Is Anomeric Retention during Collision-Induced Dissociation of Glycans? *J Am Chem Soc.* 2020;142(13):5948-5951.
24. Schaller-Duke RM, Bogala MR, Cassady CJ. Electron Transfer Dissociation and Collision-Induced Dissociation of Underivatized Metallated Oligosaccharides. *J Am Soc Mass Spectrom.* 2018;29(5):1021-1035.
25. Harvey DJ, Bateman RH, Green MR. *J Mass Spectrom.* 1997;32:167-187.
26. Yang S, Yuan W, Yang WM, et al. Glycan Analysis by Isobaric Aldehyde Reactive Tags and Mass Spectrometry. *Analytical Chemistry.* 2013;85(17):8188-8195.
27. Diedrich JK, Pinto AF, Yates JR, 3rd. Energy dependence of HCD on peptide fragmentation: stepped collisional energy finds the sweet spot. *J Am Soc Mass Spectrom.* 2013;24(11):1690-1699.
28. Diedrich JK, Pinto AFM, Yates JR. Energy Dependence of HCD on Peptide Fragmentation: Stepped Collisional Energy Finds the Sweet Spot. *J Am Soc Mass Spectr.* 2013;24(11):1690-1699.
29. Yang H, Yang CX, Sun TL. Characterization of glycopeptides using a stepped higher-energy C-trap dissociation approach on a hybrid quadrupole orbitrap. *Rapid Commun Mass Sp.* 2018;32(16):1353-1362.

30. Zhang L, Reilly JP. Extracting Both Peptide Sequence and Glycan Structural Information by 157 nm Photodissociation of N-Linked Glycopeptides. *Journal of Proteome Research.* 2009;8(2):734-742.
31. Ko BJ, Brodbelt JS. 193 nm Ultraviolet Photodissociation of Deprotonated Sialylated Oligosaccharides. *Analytical Chemistry.* 2011;83(21):8192-8200.
32. Brodbelt JS. Photodissociation mass spectrometry: new tools for characterization of biological molecules. *Chemical Society Reviews.* 2014;43(8):2757-2783.
33. Ko BJ, Brodbelt JS. 193 nm ultraviolet photodissociation of deprotonated sialylated oligosaccharides. *Anal Chem.* 2011;83(21):8192-8200.
34. Budnik BA, Haselmann KF, Elkin YN, Gorbach VI, Zubarev RA. Applications of electron-ion dissociation reactions for analysis of polycationic chitooligosaccharides in Fourier transform mass spectrometry. *Analytical Chemistry.* 2003;75(21):5994-6001.
35. Zhao C, Xie B, Chan SY, Costello CE, O'Connor PB. Collisionally activated dissociation and electron capture dissociation provide complementary structural information for branched permethylated oligosaccharides. *J Am Soc Mass Spectr.* 2008;19(1):138-150.
36. Huang YQ, Pu Y, Yu X, Costello CE, Lin C. Mechanistic Study on Electron Capture Dissociation of the Oligosaccharide-Mg2+ Complex. *J Am Soc Mass Spectr.* 2014;25(8):1451-1460.
37. Yu X, Huang YQ, Lin C, Costello CE. Energy-Dependent Electron Activated Dissociation of Metal-Adducted Permethylated Oligosaccharides. *Analytical Chemistry.* 2012;84(17):7487-7494.
38. Kornacki JR, Adamson JT, Hakansson K. Electron Detachment Dissociation of Underivatized Chloride-Adducted Oligosaccharides. *Journal of the American Society for Mass Spectrometry.* 2012;23(11):2031-2042.
39. Kailemia MJ, Park M, Kaplan DA, et al. High-Field Asymmetric-Waveform Ion Mobility Spectrometry and Electron Detachment Dissociation of Isobaric Mixtures of Glycosaminoglycans. *Journal of the American Society for Mass Spectrometry.* 2014;25(2):258-268.
40. Leach FE, Riley NM, Westphall MS, Coon JJ, Amster IJ. Negative Electron Transfer Dissociation Sequencing of Increasingly Sulfated Glycosaminoglycan Oligosaccharides on an Orbitrap Mass Spectrometer. *J Am Soc Mass Spectr.* 2017;28(9):1844-1854.
41. Wolff JJ, Leach FE, Laremore TN, et al. Negative Electron Transfer Dissociation of Glycosaminoglycans. *Analytical Chemistry.* 2010;82(9):3460-3466.
42. Han L, Costello C. Electron Transfer Dissociation of Milk Oligosaccharides. *Journal of the American Society for Mass Spectrometry.* 2011;22(6):997-1013.
43. Wei J, Wu J, Tang Y, et al. Characterization and Quantification of Highly Sulfated Glycosaminoglycan Isomers by Gated-Trapped Ion Mobility Spectrometry Negative Electron Transfer Dissociation MS/MS. *Anal Chem.* 2019;91(4):2994-3001.
44. Yu X, Jiang Y, Chen YJ, Huang YQ, Costello CE, Lin C. Detailed Glycan Structural Characterization by Electronic Excitation Dissociation. *Analytical Chemistry.* 2013;85(21):10017-10021.
45. Huang Y, Pu Y, Yu X, Costello CE, Lin C. Mechanistic Study on Electronic Excitation Dissociation of the Cellobiose-Na Complex. *J Am Soc Mass Spectrom.* 2015.
46. Tang Y, Pu Y, Gao JS, Hong PY, Costello CE, Lin C. De Novo Glycan Sequencing by Electronic Excitation Dissociation and Fixed-Charge Derivatization. *Analytical Chemistry.* 2018;90(6):3793-3801.
47. Yu Q, Wang B, Chen Z, et al. Electron-Transfer/Higher-Energy Collision Dissociation (EThcD)-Enabled Intact Glycopeptide/Glycoproteome Characterization. *J Am Soc Mass Spectrom.* 2017;28(9):1751-1764.

48. Zhang Y, Xie X, Zhao X, et al. Systems analysis of singly and multiply O-glycosylated peptides in the human serum glycoproteome via EThcD and HCD mass spectrometry. *J Proteomics.* 2018;170:14-27.
49. Zeng W, Zheng S, Su T, et al. Comparative N-Glycoproteomics Analysis of Clinical Samples Via Different Mass Spectrometry Dissociation Methods. *Front Chem.* 2022;10:839470.
50. Edge CP, R.; Rademacher, T.; Wormald, M.; Dwek, R. . *Nature.* 1992;358:693-694.
51. Franz AH, Lebrilla CB. Evidence for long-range glycosyl transfer reactions in the gas phase. *J Am Soc Mass Spectrom.* 2002;13(4):325-337.
52. Harvey DJ, Mattu TS, Wormald MR, Royle L, Dwek RA, Rudd PM. "Internal residue loss": rearrangements occurring during the fragmentation of carbohydrates derivatized at the reducing terminus. *Anal Chem.* 2002;74(4):734-740.
53. Wuhrer M, Koeleman CAM, Deelder AM. Hexose Rearrangements upon Fragmentation of N-Glycopeptides and Reductively Aminated N-Glycans. *Analytical Chemistry.* 2009;81(11):4422-4432.
54. Gao JS, Thomas DA, Sohn CH, Beauchamp JL. Biomimetic Reagents for the Selective Free Radical and Acid-Base Chemistry of Glycans: Application to Glycan Structure Determination by Mass Spectrometry. *Journal of the American Chemical Society.* 2013;135(29):10684-10692.
55. Gao JS, Jankiewicz BJ, Reece J, et al. On the factors that control the reactivity of meta-benzynes. *Chem Sci.* 2014;5(6):2205-2215.
56. Riggs DL, Hofmann J, Hahm HS, Seeberger PH, Pagel K, Julian RR. Glycan Isomer Identification Using Ultraviolet Photodissociation Initiated Radical Chemistry. *Anal Chem.* 2018;90(19):11581-11588.
57. Sohn CH, Gao JS, Thomas DA, Kim TY, Goddard WA, Beauchamp JL. Mechanisms and energetics of free radical initiated disulfide bond cleavage in model peptides and insulin by mass spectrometry. *Chem Sci.* 2015;6(8):4550-4560.
58. Turecek F, Julian RR. Peptide Radicals and Cation Radicals in the Gas Phase. *Chemical Reviews.* 2013;113(8):6691-6733.
59. Zhang X, Julian RR. Radical mediated dissection of oligosaccharides. *International Journal of Mass Spectrometry.* 2014;372:22-28.
60. Gaspar K, Fabijanczuk K, Otegui T, Acosta J, Gao JS. Development of Novel Free Radical Initiated Peptide Sequencing Reagent: Application to Identification and Characterization of Peptides by Mass Spectrometry. *J Am Soc Mass Spectr.* 2019;30(3):548-556.
61. Duan J, Kasper DL. Oxidative depolymerization of polysaccharides by reactive oxygen/nitrogen species. *Glycobiology.* 2011;21(4):401-409.
62. Harvey DJ, Mattu TS, Wormald MR, Royle L, Dwek RA, Rudd PM. "Internal residue loss": Rearrangements occurring during the fragmentation of carbohydrates derivatized at the reducing terminus. *Analytical Chemistry.* 2002;74(4):734-740.
63. Wuhrer M, Koeleman CAM, Hokke CH, Deelder AM. Mass spectrometry of proton adducts of fucosylated N-glycans: fucose transfer between antennae gives rise to misleading fragments. *Rapid Commun Mass Sp.* 2006;20(11):1747-1754.
64. Wuhrer M, Deelder AM, van der Burgt YEM. Mass Spectrometric Glycan Rearrangements. *Mass Spectrom Rev.* 2011;30(4):664-680.
65. Sturla L, Rampal R, Haltiwanger RS, Fruscione F, Etzioni A, Tonetti M. Differential terminal fucosylation of N-linked glycans versus protein O-fucosylation in leukocyte adhesion deficiency type II (CDG IIc). *Journal of Biological Chemistry.* 2003;278(29):26727-26733.
66. Ma B, Simala-Grant JL, Taylor DE. Fucosylation in prokaryotes and eukaryotes. *Glycobiology.* 2006;16(12):158r-184r.

67. Miyoshi E, Moriwaki K, Nakagawa T. Biological function of fucosylation in cancer biology. *J Biochem.* 2008;143(6):725-729.
68. Ma YL, Vedernikova I, Van den Heuvel H, Claeys M. Internal glucose residue loss in protonated O-diglycosyl flavonoids upon low-energy collision-induced dissociation. *J Am Soc Mass Spectr.* 2000;11(2):136-144.
69. Desai N, Thomas DA, Lee J, Gao JS, Beauchamp JL. Eradicating mass spectrometric glycan rearrangement by utilizing free radicals. *Chemical Science.* 2016;7(8):5390-5397.
70. Tykesson E, Mao Y, Maccarana M, et al. Deciphering the mode of action of the processive polysaccharide modifying enzyme dermatan sulfate epimerase 1 by hydrogen-deuterium exchange mass spectrometry. *Chemical science.* 2016;7(2):1447-1456.
71. Murtada R, Fabijanczuk K, Gaspar K, et al. Free-Radical-Mediated Glycan Isomer Differentiation. *Anal Chem.* 2020;92(20):13794-13802.
72. Fabijanczuk K, Gaspar K, Desai N, et al. Resin and Magnetic Nanoparticle-Based Free Radical Probes for Glycan Capture, Isolation, and Structural Characterization. *Anal Chem.* 2019;91(24):15387-15396.
73. Song XZ, Ju H, Lasanajak Y, Kudelka MR, Smith DF, Cummings RD. Oxidative release of natural glycans for functional glycomics. *Nat Methods.* 2016;13(6):528-+.

Authors:

Rayan Murtada

Rayan earned his B.S. in Biochemistry with summa cum laude at Montclair State University. With an interest in fluorescence quantitation, organic chemistry, and biochemistry, he focuses on the development and synthesis of novel tags while expanding their applications to a breadth of biomolecules (e.g., glycans, lipids, and peptides, and so forth) for rapid and accurate analyses via liquid chromatography-fluorescence detection-mass spectrometry (LC-FLD-MS). Rayan also focuses his effort on the discovery of bioconjugate fragmentation mechanisms. In the future, Rayan

seeks to pursue his MD/PhD dual-doctoral degree and applying his knowledge and research experience in the field of medicine.

Shane Finn

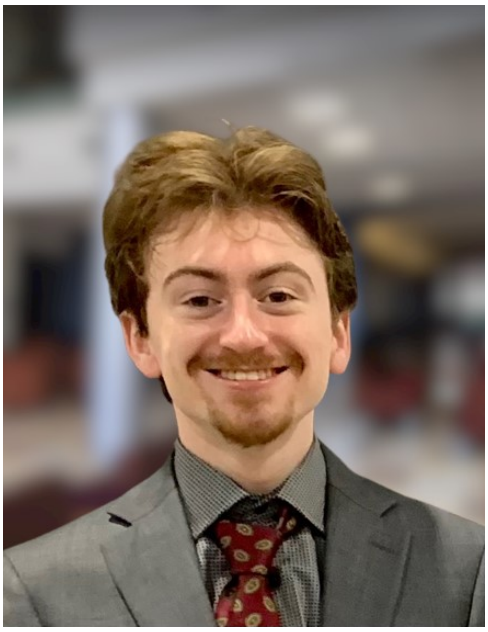

Shane will earn his B.S. in Chemistry at Montclair State University in May of 2023. Shane hopes to further his knowledge of Omics and Mass Spectrometry by pursuing a doctoral degree that will continue his analytical chemistry, organic chemistry, and biochemistry education. His efforts currently lie in the development and synthesis of novel tags that employ radical chemistry for analysis of glycans, lipids, and peptides using various mass spectrometry techniques.

Jinshan Gao

Jinshan Gao is a Professor in the Department of Chemistry and Biochemistry at Montclair State University. Dr. Gao graduated from China Agricultural University in 2005, receiving a B.S. in

Chemistry. He earned his PhD in Organic and Analytical Chemistry from Purdue University under the supervision of Dr. Hilkka I. Kenttämaa in 2012. He carried out postdoctoral research in mass spectrometric glycan analysis at the California Institute of Technology under the direction of J. L. Beauchamp before his independent research career as an Assistant Professor at Montclair State University. Supported by NSF and NIH, Dr. Gao's research interests lie in the development of free radical reagents for biomolecule characterization and quantitation, and the identification and discovery of potential biomarkers for diseases. Dr. Gao's lab has developed novel free radical fluorescence tags for simultaneous glycan quantitation and identification.